Mar Biotechnol (2012) 14:177–188
DOI 10.1007/s10126-011-9400-9

ORIGINAL ARTICLE

# The Mining of Pearl Formation Genes in Pearl Oyster *Pinctada fucata* by cDNA Suppression Subtractive Hybridization

**Ning Wang · Shigeharu Kinoshita · Naoko Nomura · Chihiro Riho · Kaoru Maeyama · Kiyohito Nagai · Shugo Watabe**

Received: 16 April 2010 / Accepted: 29 June 2011 / Published online: 19 July 2011


**Abstract** Recent researches revealed the regional preference of biomineralization gene transcription in the pearl oyster *Pinctada fucata*: it transcribed mainly the genes responsible for nacre secretion in mantle pallial, whereas the ones regulating calcite shells expressed in mantle edge. This study took use of this character and constructed the forward and reverse suppression subtractive hybridization (SSH) cDNA libraries. A total of 669 cDNA clones were sequenced and 360 expressed sequence tags (ESTs) greater than 100 bp were generated. Functional annotation associated 95 ESTs with specific functions, and 79 among them were identified from *P. fucata* at the first time. In the forward SSH cDNA library, it recognized mass amount of nacre protein genes, biomineralization genes dominantly expressed in the mantle pallial, calcium-ion-binding genes, and other biomineralization-related genes important for pearl formation. Real-time PCR showed that all the examined genes were distributed in oyster mantle tissues with a consistence to the SSH design. The detection of their RNA transcripts in pearl sac confirmed that the identified genes were certainly involved in pearl formation. Therefore, the data from this work will initiate a new round of pearl formation gene study and shed new insights into molluscan biomineralization.

**Keywords** *Pinctada fucata* · Pearl formation · Suppression subtractive hybridization · Real-time PCR

N. Wang · S. Kinoshita · N. Nomura · C. Riho · S. Watabe (✉)
Department of Aquatic Bioscience, Graduate School of Agriculture and Life Sciences, The University of Tokyo, Bunkyo, Tokyo 113-8657, Japan
e-mail: awatabe@mail.ecc.u-tokyo.ac.jp

K. Maeyama
Mikimoto Pharmaceutical CO., LTD, Ise 516-8581, Japan

K. Nagai
Pearl Research Institute, Mikimoto CO., LTD, Shima 517-0403, Japan

## Introduction

Pearl formation is a direct consequence of continuous precipitation of calcium carbonate on given nucleus with an enigmatic regulation mediated by the secretions from molluscan mantle tissues. The interplay between the organic molluscan secretions and the inorganic calcium carbonate produced the pearl layers with unique microstructural features, marvelous mechanical stiffness, and fantastic optical properties (Addadi and Weiner 1997; Addadi et al. 2006; Meyers et al. 2008; Checa et al. 2009). To understand the phenomenon of the production of iridescent pearls from their calcium carbonate building blocks, the identification and functional characterization of the organic component of the shell has been occurring for many years (Hare 1963; Towe et al. 1966; Zhang and Zhang 2006).

Almost all the possible whereabouts of the mantle secretions in molluscan species with pearl production were subjected to intensive proteomic investigations. From extrapallial fluid, nacre shell, and pearl powder, a number of important proteins have been isolated (Miyamoto et al. 1996; Sudo et al. 1997; Samata et al. 1999; Huang et al. 2007; Ma et al. 2007; Suzuki et al. 2009). Functional characterization proved their novel activities governing the precipitation, polymorph control, crystal structure modifi-

cation, and crystal growth orientation of calcium carbonate (Falini et al. 1996). The achievements of these proteomics analyses are fruitful, but the process is costly and fairly inefficient. Furthermore, because these collected data were from respective studies in different molluscan species and lacked evidence supporting their activity compatible to other species, now it still needs more information to sketch a full picture of the mechanism involved in pearl formation.

Alternatively, the molecular cloning of gene transcripts in mantle tissues allows the identification of hundreds of genes in one cDNA library and makes full use of the relevant information in prior researches to discover novel genes. Especially, the techniques of suppression subtractive hybridization (SSH) hold great promises to increase the cDNA library specificity in isolation of target genes, only if these genes are in differential transcript abundances between two experimental samples (Diatchenko et al. 1996).

Recently, the regional differential transcription of biomineralization genes in the mantle of *Pinctada fucata* was reported (Wang et al. 2009). Both in situ hybridization and real-time PCR revealed that mantle pallial dominantly transcribed most of the known genes responsible for aragonite precipitation on nacreous layer of shell or pearl biogenesis, while mantle edge got more expression of genes directing the calcite shell growth of oysters (Takeuchi and Endo 2006).

Therefore, the present study employed this differential expression of pearl formation genes in mantle regions to construct the SSH cDNA libraries for the identification of regulatory genes for oyster pearl formation. Both the forward and reverse SSH between the cDNAs from mantle pallial and mantle edge of pearl oyster, *P. fucata*, were conducted to screen the important genes specific to each mantle region. Totally, 669 clones were sequenced and subjected to the functional annotation by blast analysis and gene ontology clustering. To validate the SSH efficiency in this study, the expression of representative genes in mantle pallial and mantle edge of oysters was examined by real-time PCR. The potential contribution of the representative genes from mantle pallial SSH cDNA library to pearl formation was confirmed by the presence of their RNA transcripts in the pearl-secreting tissue, which was termed as "pearl sac".

## Materials and Methods

### Experimental Animals

Adult pearl oyster *P. fucata* with an average shell length of 9.8±1.0 cm were collected from an oyster aquaculture farm of Mikimoto Pearl Co. Ltd (Mie Prefecture, Japan) in summer (July 1st, 2008). In order to avoid unnecessary stimulations during transportation or by culture environment changes, all the live specimens were sacrificed on site. Animal anatomy and tissue sampling were similar to our previous report (Wang et al. 2009). Specifically, the regional discrimination of oyster mantle pallial and mantle edge followed the same way as the preparation of donor tissues in pearl aquaculture (Gong et al. 2008). From pearl aquaculture oysters with a similar body size, tissues composed of the thin cell layers surrounding an aquaculture pearl were carefully isolated from the gonad part and used as the pearl sac for further experiments. All the pearl sac samples were collected from oysters subjected to nucleus implantation on July 1st, 2007, since they certainly produced pearls with a high-speed growth in oysters at 1 year after nucleus implantation, according to our empirical observations. The dissected samples were swiftly frozen by liquid nitrogen and stored at −80°C until use.

### RNA Extraction

Total RNAs were carefully extracted from pearl oyster mantle edge, mantle pallial, and pearl sac using an Isogen RNA extraction kit (Nippon Gene, Toyama, Japan) according to the kit manual. To remove a possible genomic DNA contamination, the isolated RNA was treated with Turbo DNA-free™ (Applied Biosystems, Foster City, CA, USA) at 37°C for 1 h. The integrity of RNA was checked by electrophoresis on a 1% formaldehyde-denatured agarose gel. For SSH library construction, mRNA was purified by loading the total RNA from oyster mantle edge or mantle pallial through the Oligotex-dT 30 resin column (Takara, Otsu, Japan). The concentration of RNA was determined by measuring optical density at 260 nm with a DU530 Life Science UV-visible spectrophotometer (Beckman Coulter, Fullerton, CA, USA).

### Construction of the Mantle Pallial and Mantle Edge SSH Libraries

First of all, mantle edge or mantle pallial mRNA from three oysters were mixed as the RNA pools to minimize the fluctuation of the composite RNA abundance resulting from different oyster individuals. With 2 μg of mRNA from each RNA pool, cDNAs of mantle edge and mantle pallial were synthesized and subjected to SSH using a PCR-Selected TM cDNA Subtraction Kit (Clontech, Mountain View, CA, USA). In the forward SSH, mantle pallial cDNA was used as the "tester" and mantle edge cDNA as the "driver", while the reverse SSH used these cDNAs in an opposite way. In brief, after endonuclease digestion, the tester cDNA was divided into two parts, and one was ligated to adaptor 1 and the other to adaptor

2R (both provided in the kit). During the first hybridization, an excess of driver cDNA (without adaptors) was added to each tester pool. In the second hybridization, the two primary hybridization reactions were mixed together without denaturation, and freshly denatured driver cDNAs were added to further enrich differentially expressed fragments. The unsubtracted tester control was prepared using the same procedures but without the subtractive hybridization step. Subsequently, two PCR amplifications were performed to suppress the background cDNAs and enrich the target sequences. The PCR products were fractionated by a Chroma spin™100 column (Clontech) to remove the cDNA fragments smaller than 100 bp. The purified PCR products were cloned into the pGEM-T vector (Promega, Madison, WI, USA) and transformed into *Escherichia coli* JM109 competent cells by heat shock. In the last, both the forward and reverse SSH libraries were plated on Luria-Bertani agar plates supplemented with 100 μg/ml ampicillin, 20 mg/cm$^2$ X-gal, and 12.1 mg/cm$^2$ isopropyl β-D-1-thiogalactopyranoside. All the attained cDNA colonies were sequenced by using an ABI prism 3100 genetic analyzer (Applied Biosystems).

## Sequence Analysis

The sequence data were mass-aligned with the vector by using DNAssist 2.0 and the sequences homologous to the vector or adaptor were trimmed. The low-quality data or the sequence with a length less than 100 bp was discarded manually. The trimmed sequences were used for contig assembly by using a web interface of the CAP3 software (http://deepc2.psi.iastate.edu/aat/cap/cap.html) (Huang and Madan 1999). The properly assembled contigs or singletons were used to blast against the non-redundant database of National Center for Biotechnology Information (NCBI; http://www.ncbi.nlm.nih.gov/BLAST). The best-annotated hit from the similarity search was retained. Novel sequences were submitted to the DNA Data Bank of Japan and accession numbers were assigned from FS940938 to FS941297. Gene ontology (GO) annotation was assigned by using AmiGO against the GO database (http://amigo.geneontology.org/cgi-bin/amigo/go.cgi). The expressed sequence tag datasets (ESTs) specific for mantle pallial were systematically analyzed by Blast2GO to get an overview of gene categories involved in nacre secretion.

## Validation of Differential Gene Expression by Quantitative Real-Time PCR

The present SSH efficiency in the elimination of redundant RNA transcripts was examined by the comparison of the differential expression of a housekeeping gene encoding *P. fucata* elongation factor 1 alpha (EF1α) in the mantle pallial cDNA tester with or without SSH. To validate the fidelity of the present SSH, the representative genes from the two SSH cDNA libraries were selected to compare their RNA transcript abundance in mantle pallial and mantle edge of oysters. The expression of the selected genes from mantle pallial SSH cDNA library in pearl sac was also detected by the quantitative real-time PCR. Specific oligo primer pairs were designed for these test genes and their PCR efficiency was determined by running standard curves for 10-fold serial dilutions of cDNA templates (Table 1). The used template cDNAs were synthesized by using 2 μg total RNA from mantle edge, mantle pallial, and pearl sac with SuperScript III reverse transcriptase (Invitrogen, Carlsbad, CA, USA) in accordance with the user manual provided by the manufacturer.

Quantitative real-time PCR analyses were then performed using a thermal cycler 7300 Real-Time PCR System (Applied Biosystems) equipped with a 96-well plate system with the SYBR green premix ExTaqII kit (Takara). All real-time PCR experiments were performed with three independent sets of RNA samples: each analysis was performed in a final volume of 20 μl containing 10 μM each of forward and reverse primers, 1 μl diluted template cDNA (about 10 ng), and 0.4 μl 6-carboxyl-X-rhodamine reference dye. The following thermal cycling profile was used for all PCRs: 95°C for 20 s, 40 cycles of 95°C for 10 s, and 60°C for 1 min. The absence of nonspecific products was confirmed by dissociation curve analysis (60°C to 95°C). Fluorescence was monitored at the end of each cycle to obtain the amount of PCR products. The point at which the SYBR fluorescent signal was statistically significant above background was defined as the cycle threshold (Ct), the optimal value of which was chosen automatically. Finally, the real-time PCR results were represented as the relative expression levels of target genes to those of reference genes. Glyceraldehydes-3-phosphate dehydrogenase gene was selected as the housekeeping reference gene in this study, since it was demonstrated as a reliable control in biomineralization gene expression studies (Takeuchi and Endo 2006; Wang et al. 2009). To exclude the variation caused by different PCR efficiency, the relative expression levels were calculated by using the following equation based on the gene expression's Ct difference method (Schefe et al. 2006): relative mRNA expression level $= \frac{E_{\mathrm{HKG}}{}^{\mathrm{CT\,HKG}}}{E_{\mathrm{GOI}}{}^{\mathrm{CT\,GOI}}}$, where $E_{\mathrm{HKG}}$ and $E_{\mathrm{GOI}}$ are the PCR efficiencies and $\mathrm{CT_{HKG}}$ and $\mathrm{CT_{GOI}}$, the threshold cycles for the reference housekeeping gene and a given interest gene, respectively. For the differential gene expression analysis among various samples, statistical analyses were manipulated by using one-way analysis of variance followed by Tukey's test in Sigma Plot 10.0 (SYSTAT, Chicago, IL, USA). Data were represented as

**Table 1** Real-time PCR primers used in the present study

| Gene | | Sequence | Accession number | Amplicon size (bp) | PCR efficiency |
|---|---|---|---|---|---|
| AP24 LP | F | TGCACGGAAGAACCGAACAC | FS941098 | 121 | 1.90 |
| | R | TTACCACAGCATCTTTAACAAGTCC | | | |
| EF1α | F | GGCCACAGAGATTTCATCAAGAAC | AB205403 | 82 | 2.08 |
| | R | CAACACCAGCAGCAATAATCAACAC | | | |
| ELP | F | AGTTGGAGGCTTTGGTGTTCC | FS941290 | 159 | 1.92 |
| | R | CCGGCAAGGTCTAGTCCGTAT | | | |
| FLP | F | CGCCAGTTACACCTATCAGTCA | FS941085 | 72 | 2.10 |
| | R | TTGGCAAATCCTGGTAGAGC | | | |
| Fibulin | F | AAGTTCAGTGTCAGCAGGGTTAC | FS941195 | 96 | 1.97 |
| | R | TTCCTCGGCTATCGGCTTGTC | | | |
| GAPDH | F | AAATGGGAAGTTGACAGGAATGGC | AB205404 | 52 | 1.98 |
| | R | CGAAACATCAGATACAGGCACACG | | | |
| Lustrin A LP | F | CCTATCACAGCACACTCCGTTTC | FS941194 | 105 | 1.90 |
| | R | AGACCTATTGGCAGACCAGACAG | | | |
| Mantle gene 6 | F | TTTGCCTGCATGTGATTTCC | FS941090 | 146 | 1.90 |
| | R | CTGAGCCATTACCGTCTTCG | | | |
| Neogenin | F | ACTGCACTTCCGGCACCAG | FS941217 | 157 | 1.94 |
| | R | TAAACTACACTGACAGTCGCTACACC | | | |
| Perlwapin LP | F | AGACAAACAAGCCATACAAGAAACC | FS941021 | 154 | 1.97 |
| | R | TCCACGCCCTGACGAGATAATAC | | | |
| SPI | F | GACATCTTCCTTTAGAGCGAACTTC | FS941243 | 104 | 1.99 |
| | R | CACTCTTCAGTATGATCCTGTTTGC | | | |
| TCP | F | AGTCATAGGCAAACACAGGAATGG | FS941211 | 95 | 1.90 |
| | R | CGGAGTCAACTTCTACTTTGGTTCG | | | |

PCR efficiencies ($E$) were calculated according to the equation $E=10^{-1/\text{slope}}$

*AP24* aragonitic protein 24 kDa-like protein, *EF1α* elongation factor 1 alpha, *ELP* extensin-like protein, *FLP* ferritin-like protein, *GAPDH* glyceraldehydes-3-phosphate dehydrogenase, *Lustrin A LP* Lustrin-A-like protein, *Perlwapin LP* Perlwapin-like protein, *SPI* serine proteinase inhibitor, *TCP* thioester-containing protein

the mean ± standard error of the mean ($n=3$), and the differences were considered significant at $P<0.05$.

## Results

### Gene Identification from the SSH cDNA Libraries

A total of 428 clones of the mantle pallial SSH cDNA library and 241 clones of the mantle edge SSH cDNA library were sequenced from the 5′ end, resulting in the characterization of 360 ESTs with sizes greater than 100 bp after the elimination of vector sequences. Following the redundancy analysis with CAP3, non-redundant contigs or singletons were assembled and then aligned against the Blastx and tBlastX databases in NCBI for functional annotation. There were 104 contigs or singletons showing no hits, or hits to hypothetical proteins or sequences without functional association. The rest ESTs showed a high similarity with 95 genes with identifiable functions, which covered 16 genes from *P. fucata* and the rest 79 genes in the first time identification in this animal species (Tables 2, 3, 4). Among these identifiable ESTs, 45 genes were exclusively present in mantle pallial SSH cDNA library (Table 2), while 25 genes were specific to mantle edge SSH cDNA library (Table 3). There are 25 genes, which were present in both the mantle pallial and mantle edge SSH cDNA libraries (Table 4). It is noteworthy to point out that three homologous genes of nacreous shell matrix proteins (labeled by superscript a in Tables 2 and 3) were detected in the present cDNA libraries.

### Gene Ontology Analysis of the Genes from MP SSH Library

The computational analysis of the whole EST collection using the software Blast2GO allowed the annotation of the expressed sequences according to three terms of the gene ontology analysis: cellular component, molecular function, and biological process (Fig. 1). Concerning the molecular function, the most represented categories were those of protein binding and ion binding, followed by nucleotide binding and hydrolase activity (Fig. 1a). The other molecular functions were represented at a lower extent.

**Table 2** Genes exclusively identified from the mantle pallial suppression subtractive hybridization cDNA library

| | Accession number | Size (bp) | Homologous gene | Animal resource | *E* value | Similarity (%) | GO ID | GO description |
|---|---|---|---|---|---|---|---|---|
| 1 | FS941098 | 295 | Aragonite protein 24 kDa (AP24)[a] | *Haliotis rufescens* | 1.60E-00 | 31 | Unknown | |
| 2 | FS941214 | 363 | EF hand calcium-binding protein[b] | *Pinctada fucata* | 4.00E-29 | 82 | GO:0005509 | Calcium ion binding |
| 3 | FS941195 | 260 | Fibulin-1 precursor | *Brugia malayi* | 6.00E-13 | 39 | GO:0005509 | Calcium ion binding |
| 4 | FS941171 | 360 | Mantle gene 4[a] | *Pinctada fucata* | 8.00E-18 | 93 | Unknown | |
| 5 | FS941090 | 400 | Mantle gene 6[a] | *Pinctada fucata* | 5.00E-04 | 31 | GO:0005509 | Calcium ion binding |
| 6 | FS941151 | 164 | Mantle protein 11[a] | *Pinctada fucata* | 1.00E-15 | 100 | Unknown | |
| 7 | FS941068 | 286 | Nacrein[a] | *Pinctada fucata* | 9.00E-08 | 65 | Unknown | |
| 8 | FS941247 | 264 | Calcium-ion-binding protein | *Ricinus communis* | 2.50E-02 | 63 | GO:0005509 | Calcium ion binding |
| 9 | FS941113 | 336 | Ovoperoxidase | *Lytechinus variegatus* | 6.00E-11 | 37 | GO:0005509 | Calcium ion binding |
| 10 | FS941226 | 359 | S100 calcium-binding protein A10b | *Danio rerio* | 2.80E-01 | 36 | GO:0005509 | Calcium ion binding |
| 11 | FS941114 | 385 | Paramyosin | *Mytilus galloprovincialis* | 3.00E-43 | 84 | GO:0005488 | Binding |
| 12 | FS941217 | 288 | Neogenin | *Gallus gallus* | 9.00E-05 | 30 | GO:0045296 | Cadherin binding |
| 13 | FS941111 | 332 | Neogenin homolog 1 | *Homo sapiens* | 3.00E-06 | 29 | GO:0045296 | Cadherin binding |
| 14 | FS941131 | 366 | Chromobox-like 7 | *Homo sapiens* | 4.00E-03 | 56 | GO:0003682 | Chromatin binding |
| 15 | FS941264 | 351 | Beta tubulin | *Cimex lectularius* | 1.00E-25 | 98 | GO:0005525 | GTP binding |
| 16 | FS941224 | 352 | Beta tubulin | *Halocynthia roretzi* | 1.00E-57 | 97 | GO:0005525 | GTP binding |
| 17 | FS941231 | 391 | Dual oxidase 1 | *Lytechinus variegatus* | 9.00E-31 | 55 | GO:0005506 | Iron ion binding |
| 18 | FS941097 | 353 | Phenylalanine ammonia-lyase | *Ginkgo biloba* | 1.00E-17 | 55 | GO:0016829 | Lyase activity |
| 19 | FS941116 | 334 | Not-like transcription complex | *Brugia malayi* | 4.00E-03 | 82 | GO:0046872 | Metal ion binding |
| 20 | FS941139 | 433 | Ubiquinol-cytochrome c reductase core protein II | *Danio rerio* | 7.00E-06 | 39 | GO:0046872 | Metal ion binding |
| 21 | FS941091 | 348 | Nucleoside diphosphate kinase B | *Haliotis discus discus* | 2.00E-24 | 75 | GO:0005515 | Protein binding |
| 22 | FS941286 | 296 | Polyubiquitin | *Artemia franciscana* | 6.00E-25 | 82 | GO:0005515 | Protein binding |
| 23 | FS941290 | 368 | Extensin-like protein | *Zea mays* | 9.00E-04 | 44 | GO:0005515 | Protein binding |
| 24 | FS941256 | 350 | Putative ubiquitin/40S ribosomal protein RPS27A fusion protein | *Novocrania anomala* | 1.00E-22 | 97 | GO:0005515 | Protein binding |
| 25 | FS941259 | 228 | Ubiquitin C | *Schistosoma japonicum* | 3.00E-34 | 98 | GO:0005515 | Protein binding |
| 26 | FS941297 | 399 | Alpha 3 type VI collagen | *Homo sapiens* | 2.00E-06 | 54 | GO:0005515 | Protein binding |
| 27 | FS941165 | 341 | Activated T-cell marker CD109 | *Homo sapiens* | 2.20E-02 | 35 | GO:0005515 | Protein binding |
| 28 | FS941129 | 343 | SREB transcription factor | *Saccoglossus kowalevskii* | 1.00E-23 | 48 | GO:0005515 | Protein binding |
| 29 | FS941281 | 318 | Poly(A)-binding protein | *Spisula solidissima* | 8.00E-11 | 91 | GO:0008022 | Protein C terminus binding |
| 30 | FS941265 | 344 | 67 kD laminin receptor precursor | *Pinctada fucata* | 8.00E-37 | 100 | GO:0004872 | Receptor activity |
| 31 | FS941272 | 257 | Receptor of activated kinase C | *Crassostrea angulata* | 3.00E-41 | 93 | GO:0004872 | Receptor activity |
| 32 | FS941283 | 310 | Tubulin alpha 8-like 3b | *Danio rerio* | 7.00E-15 | 99 | GO:0005524 | Receptor activity |
| 33 | FS941295 | 120 | Receptor of activated kinase C | *Crassostrea angulata* | 3.00E-07 | 68 | GO:0003908 | S-methyltransferase activity |
| 34 | FS941291 | 293 | Galectin | *Pinctada fucata* | 4.00E-46 | 98 | GO:0005529 | Sugar binding |
| 35 | FS941241 | 353 | Novel protein containing a galactose binding lectin domain | *Danio rerio* | 2.00E-17 | 54 | GO:0005529 | Sugar binding |
| 36 | FS941126 | 622 | Kazal-type serine proteinase inhibitor | *Chlamys farreri* | 1.00E-32 | 45 | GO:0004867 | Sugar binding |
| 37 | FS941273 | 398 | Rhamnose-binding lectin OLL | *Spirinchus lanceolatus* | 7.00E-17 | 42 | GO:0005529 | Sugar binding |
| 38 | FS941243 | 354 | Serine protease inhibitor CFSPI3 | *Chlamys farreri* | 8.00E-29 | 60 | GO:0004867 | Sugar binding |
| 39 | FS941215 | 379 | Cytochrome oxidase subunit 2 | *Ariosoma shiroanago* | 1.00E-13 | 46 | GO:0046914 | Transition metal ion binding |
| 40 | FS941094 | 356 | Leukocyte-antigen-related-like | *Drosophila melanogaster* | 2.00E-07 | 33 | GO:0005001 | Transmembrane receptor protein tyrosine phosphatase activity |

**Table 2** (continued)

| | Accession number | Size (bp) | Homologous gene | Animal resource | *E* value | Similarity (%) | GO ID | GO description |
|---|---|---|---|---|---|---|---|---|
| 41 | FS941262 | 235 | Adenine nucleotide translocator precursor | *Zea mays* | 5.00E-07 | 82 | Unknown | |
| 42 | FS941277 | 133 | Lysine-rich matrix protein-4 | *Pinctada fucata* | 5.00E-09 | 100 | Unknown | |
| 43 | FS941156 | 361 | Regeneration-upregulated protein 3 | *Enchytraeus japonensis* | 1.00E-05 | 31 | Unknown | |
| 44 | FS941269 | 252 | S-adenosyl-L-homocysteine hydrolase | *Dictyostelium discoideum AX4* | 4.00E-37 | 86 | Unknown | |
| 45 | FS941211 | 288 | Thioester-containing protein | *Chlamys farreri* | 1.00E-06 | 40 | Unknown | |

[a] Oyster and abalone nacreous shell matrix protein genes (Miyamoto et al. 1996; Michenfelder et al. 2003)

[b] Biomineralization genes in oysters (Liu et al. 2007)

When the term of cellular component was concerned, the most represented were intracellular, intracellular part, intracellular organelle, and intracellular organelle part with about 55% of the total annotations, followed by membrane,

**Table 3** Genes exclusively identified from the mantle edge suppression subtractive hybridization cDNA library

| | Accession number | Size (bp) | Homologous gene | Animal resource | *E* value | Similarity (%) |
|---|---|---|---|---|---|---|
| 1 | FS940999 | 510 | Aspein[a] | *Pinctada fucata* | 7.00E-58 | 96 |
| 2 | FS941085 | 350 | Ferritin-like protein[a] | *Pinctada fucata* | 4.00E-38 | 100 |
| 3 | FS941194 | 284 | Lustrin A[b] | *Haliotis rufescens* | 7.00E-04 | 42 |
| 4 | FS941021 | 410 | Perlwapin[b] | *Haliotis laevigata* | 4.10E-01 | 38 |
| 5 | FS940996 | 446 | Shematrin-1[b] | *Pinctada fucata* | 7.00E-09 | 98 |
| 6 | FS941123 | 451 | Shematrin-2[b] | *Pinctada fucata* | 5.00E-10 | 100 |
| 7 | FS941035 | 507 | Tyrosinase[b] | *Pinctada fucata* | 4.00E-66 | 100 |
| 8 | FS940948 | 677 | Bromodomain containing 4 isoform 1 | *Mus musculus* | 9.60E-01 | 40 |
| 9 | FS940955 | 510 | Catalase | *Campylobacter jejuni* | 6.00E-09 | 96 |
| 10 | FS940944 | 544 | CCAAT enhancer binding protein | *Lehmannia valentiana* | 7.00E-07 | 50 |
| 11 | FS940951 | 419 | CCAAT/enhancer binding protein | *Haliotis diversicolor* | 3.00E-21 | 71 |
| 12 | FS941006 | 439 | Chicken cytotactin 200 kD | *Gallus gallus* | 6.00E-07 | 42 |
| 13 | FS941012 | 159 | Collagen | *Monitor capitata* | 2.00E-07 | 46 |
| 14 | FS940968 | 239 | Fructose dehydrogenase small subunit | *Gluconobacter frateurii* | 2.00E-03 | 88 |
| 15 | FS940950 | 731 | Fibronectin type III domain containing 1 | *Homo sapiens* | 9.00E-05 | 48 |
| 16 | FS941036 | 283 | KRMP3 gene for lysine-rich matrix protein 3 | *Pinctada fucata* | 7.00E-03 | 72 |
| 17 | FS940938 | 288 | KRMP-10 mRNA | *Pinctada margaritifera* | 2.00E-03 | 66 |
| 18 | FS940946 | 502 | Heat shock protein 70 | *Helicoverpa zea* | 5.00E-22 | 70 |
| 19 | FS941025 | 263 | Hemagglutinin esterase | *Infectious salmon anemia virus* | 7.00E-04 | 82 |
| 20 | FS941042 | 245 | Lipoxygenase | *Capsicum annuum* | 7.00E-04 | 75 |
| 21 | FS940985 | 453 | Neuropeptide receptor A32 | *Bombyx mori* | 1.00E-10 | 68 |
| 22 | FS940970 | 223 | Putative DNA methyltransferase | *Enterobacteria phage T4* | 2.00E-03 | 64 |
| 23 | FS941026 | 246 | Profilin | *Strongylocentrotus purpuratus* | 3.00E-07 | 50 |
| 24 | FS940975 | 455 | Serase-1B | *Homo sapiens* | 2.00E-14 | 57 |
| 25 | FS940959 | 449 | Vitelline membrane outer layer 1 homolog precursor | *Mus musculus* | 4.00E-17 | 39 |

[a] Biomineralization genes in oysters (Zhang et al. 2003; Zhang et al. 2006; Yano et al. 2006; Takeuchi et al. 2008)

[b] Abalone nacre protein genes (Shen et al. 1997; Treccani et al. 2006)

**Table 4** Common genes identified from mantle pallial and mantle edge suppression subtractive hybridization cDNA libraries

| | Accession number | Size (bp) | Homologous gene | Animal resource | *E* value | Similarity (%) |
|---|---|---|---|---|---|---|
| 1 | FS941238 | 363 | Actin | *Pinctada fucata* | 3.00E-51 | 97 |
| 2 | FS941092 | 317 | Elongation factor 1 alpha | *Axinella verrucosa* | 8.00E-24 | 95 |
| 3 | FS940954 | 461 | Elongation factor 1 alpha | *Ircinia strobilina* | 8.00E-56 | 86 |
| 4 | FS941199 | 327 | Eukaryotic translation initiation factor 4A | *Callinectes sapidus* | 2.00E-39 | 90 |
| 5 | FS940983 | 473 | Elongation factor-1, delta, b isoform 1 | *Danio rerio* | 3.00E-35 | 77 |
| 6 | FS941013 | 479 | Mitochondrial gene for 16S rRNA | *Pinctada fucata* | 4.00E-88 | 100 |
| 7 | FS941147 | 297 | Putative 60S ribosomal protein RPL7A | *Novocrania anomala* | 2.00E-34 | 90 |
| 8 | FS941255 | 315 | Ribosomal protein | *Mytilus galloprovincialis* | 1.00E-41 | 81 |
| 9 | FS941115 | 217 | Ribosomal protein 3 large subunit | *Priapulus caudatus* | 1.00E-25 | 87 |
| 10 | FS941124 | 235 | Ribosomal protein S4 | *Argopecten irradians* | 4.00E-19 | 88 |
| 11 | FS941128 | 258 | Ribosomal protein L5 | *Argopecten irradians* | 4.00E-31 | 80 |
| 12 | FS941121 | 300 | Ribosomal protein rpl7a | *Arenicola marina* | 3.00E-28 | 83 |
| 13 | FS941109 | 270 | Ribosomal protein rpl10a | *Lineus viridis* | 3.00E-21 | 74 |
| 14 | FS941093 | 376 | Ribosomal protein S15 | *Argopecten irradians* | 1.00E-46 | 91 |
| 15 | FS941154 | 194 | Ribosomal protein L18 | *Crassostrea gigas* | 3.00E-24 | 87 |
| 16 | FS941169 | 298 | Ribosomal protein L19 | *Ixodes scapularis* | 1.00E-33 | 88 |
| 17 | FS941216 | 270 | Ribosomal protein rps21 | *Eurythoe complanata* | 2.00E-16 | 82 |
| 18 | FS941140 | 308 | Ribosomal protein S26 | *Octopus vulgaris* | 1.00E-37 | 91 |
| 19 | FS941166 | 236 | Ribosomal protein L28 | *Haliotis asinina* | 1.00E-06 | 71 |
| 20 | FS940973 | 285 | 40S ribosomal protein S29 | *Caligus rogercresseyi* | 3.00E-03 | 94 |
| 21 | FS941001 | 286 | 40S ribosomal protein S29 | *Ornithodoros parkeri* | 2.00E-11 | 85 |
| 22 | FS941144 | 210 | Putative ribosomal protein L31 | *Sipunculus nudus* | 3.00E-31 | 91 |
| 23 | FS941157 | 279 | Ribosomal protein rpl35a | *Lineus viridis* | 3.00E-39 | 81 |
| 24 | FS941158 | 292 | 40S ribosomal protein S2 | *Ictalurus punctatus* | 2.00E-22 | 79 |
| 25 | FS941172 | 285 | 40S ribosomal protein S3a | *Haliotis diversicolor* | 9.00E-31 | 94 |

membrane-bounded organelle, membrane part, and non-membrane-bounded organelle (Fig. 1b). The endomembrane system and extracellular space were only present as 3% of all the cellular component annotation.

In view of biological process, the analyzed genes for this gene ontology study could be involved in 16 vocabularies, such as cellular process, metabolic process, and so on (Fig. 1c). Biological regulation, regulation of biological process, positive regulation of biological process, and negative regulation of biological process together presented the biggest share of all the terms in biological process (23 of 91). Although numerically less represented, it is worth to mention the presence of terms related to biological adhesion and immune response.

### The Efficiency of SSH

To test the suppression of redundant genes in the SSH cloning, the abundance of EF1$\alpha$ transcripts in mantle edge and mantle pallial tester cDNA libraries were quantitatively compared and a reduction of 1,652-fold was detected on average (Fig. 2). Furthermore, the real-time PCR analyses validated the results from SSH experiments for 10 genes, which were specific to mantle pallial or mantle edge SSH cDNA library (Tables 1 and 2). All the selected genes showed significant differential expression in mantle pallial and mantle edge corresponding to their library specificity (Figs. 3 and 4). In addition, the expression of specific genes in pearl sac was also detected (Fig. 3). Most of the genes showed lower expression levels in pearl sac. Remarkably, the serine proteinase inhibitor gene showed higher expression levels in pearl sac than reference mantle pallial.

## Discussion

*P. fucata* is famous for the production of high-quality akoya pearls with pearl output accounting for more than 85% of the world. The pearl formation of oyster mainly is attributed to its mantle pallial tissues according to the morphological observation. Molluscan shell formation is accomplished by an accretionary growth way and calcium carbonate precipitation occurs more actively in the distal than proximal region (Che et al. 2001; Rousseau et al. 2005). Furthermore, mantle

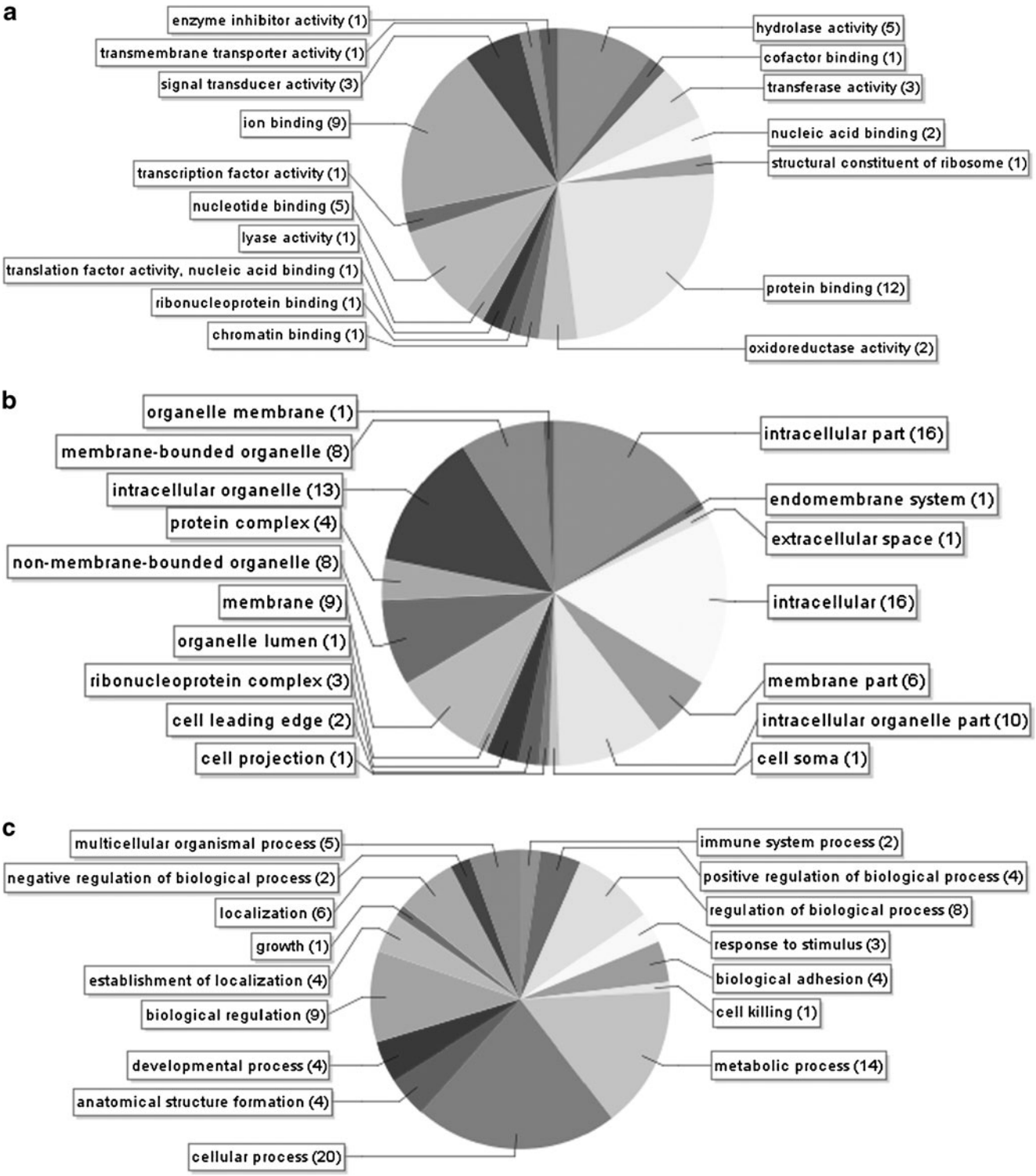


**Fig. 1** GO term distribution of ESTs specific for mantle pallial SSH cDNA library. GO categories are provided in the molecular function (**a**), cellular components (**b**), and biological process vocabularies (**c**). ESTs without annotation are not included in this analysis

pallial just covers the nacreous shells, which are structurally identical to pearls. Therefore, proteins from mantle pallial may participate in the nacre secretion in a real time. Pearl aquaculture convincingly supports this, since a piece of oyster mantle pallial with an appropriate transplantation surgery may develop into a pearl sac and give a birth to a pearl. The present study employed the SSH technique to generate cDNAs with dominant expressions in mantle pallial

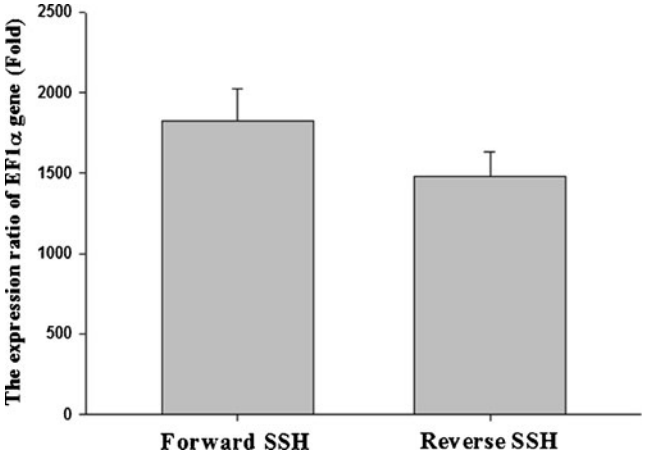


**Fig. 2** The redundant gene suppression efficiency of mantle pallial and mantle edge SSH cDNA libraries. The mRNA expression ratio of the EF1α gene = $E_{EF1\alpha}^{\triangle CT}$. $E_{EF1\alpha}$ refers to the PCR efficiency of the used primer; $\triangle$CT is the cycle threshold value difference between unsubtracted and subtracted tester cDNAs in real-time PCR reactions

and thereby to discover the regulatory genes with high association to the pearl biogenesis.

The cDNA SSH between the two regions of pearl oyster mantle successfully reduced the presence of redundant housekeeping genes in cDNA libraries. The EF1α gene expression levels in SSH cDNAs were more than 1,500-fold lower than those of the reference cDNAs without SSH. This indicates the success of the present SSH and enrichment of the target genes in a high cloning efficiency. However, the SSH technique cannot eliminate all the redundant cDNAs, if the gene expression is in low abundance or less quantitatively different between two hybridized samples (Diatchenko et al. 1999). Therefore, both the forward and reverse SSHs were processed in this study. ESTs with concurrent to two direction SSHs could be discarded as the background of SSH. The genes without library specificity in this study were separately listed in Table 4. By this way, the genes with differential expression could be faithfully separated. The following real-time PCR results confirmed the fidelity of the present SSH that the selected genes displayed significant differential expression in oyster mantle edge and mantle pallial in consistence with their specificity for their representative cDNA libraries.

With the construction of two cDNA libraries, a total of 95 genes were discovered at one time. The 83% genes were in the first identification from pearl oyster. This exhibited the excellent efficiency of the SSH cDNA libraries in the gene identification and novel gene discovery. It seems that the present SSH cDNA library is not in a big scale. However, it should be not always appropriate to evaluate the efficiency of a cDNA library by its numbers of clone or non-redundant ESTs since the destination of SSH is to enrich the cloning efficiency of genes with specific interests and this accompanies the exclusion of a large amount of non-target genes, while a normal EST library will contain most of the genes in sample tissues without discrimination of the functional characters of genes (Straub et al. 2004; Sanchez et al. 2007; Perrigault et al. 2009; Roberts et al. 2009; Xu and Faisal 2009). Therefore, the comparative efficiency of a SSH cDNA library should depend on the numbers of identifiable genes, which practice the aim of the library construction. Previously, the cDNA library with a SSH between mantle and muscle in *Pinctada margaritifera* collected 72 unique ESTs and six of them were functionally identifiable (Duplat et al. 2006). In *P. fucata*, a similar SSH cDNA library identified 10 novel genes (Liu et al. 2007). Compared with these works, the SSH cDNA libraries in this study approached great success.

In the subsequent functional annotation analysis, the ESTs identified in this work showed high homology with four important nacreous shell matrix protein genes, four biomineralization genes with dominant expression in pearl oyster mantle pallial, and other 34 candidate biomineralization-related genes for pearl formation. First of all, proteins extracted from molluscan pearl or nacreous shell matrix definitely are responsible for nacre constitution and their functional studies demonstrated their pivotal regulation in pearl formation and refreshed the understanding of the biomineralization. In *P. fucata*, hitherto less than 10 nacreous shell matrix proteins have been reported (Suzuki et al. 2009; Wang et al. 2009). The most well-known protein is nacrein, which is characterized as a ubiquitous enzyme catalyzing the acidification of $CO_2$ to form $HCO_3^-$ and thereby controlling the calcium carbonate accumulation for pearl growth (Miyamoto et al. 1996). Besides the nacrein, three more novel genes with sequence similarity to those encoding abalone nacre proteins, aragonetic protein 24 kDa (AP24), lustrin A, and perlwapin, were identified from this work. We designated them as AP24, lustrin A, and pearlwapin-like protein gene. It had been demonstrated that the abalone AP24 may bind to calcium carbonate at crystal growth steps, promoting calcium carbonate to form aragonite for pearl formation instead of calcite shell growth (Michenfelder et al. 2003). Abalone lustrin A has been believed to play important roles in the interaction with the polyanionic aragonite-determining proteins, protecting the protein components of nacre from degradation, and conferring elastic resiliency (Shen et al. 1997). As for abalone perlwapin, it possessed whey acidic protein domain and could inhibit the growth of calcium carbonate crystals. In another word, perlwapin could be an important factor regulating the speed of pearl growth (Treccani et al. 2006). All of these suggest that the further characterization of these three genes is of marvelous interests revealing the differential nacre formation mechanisms among molluscans and to determine the most conserved

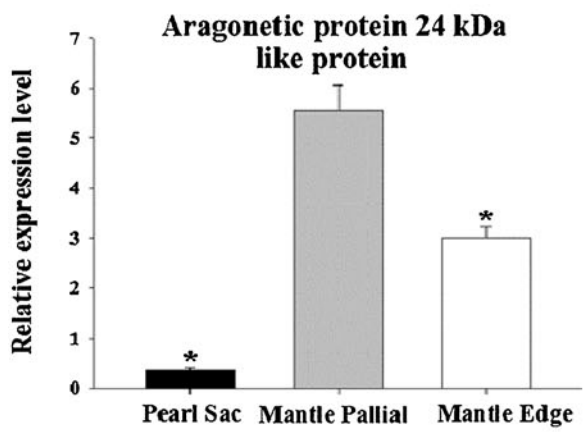
Aragonetic protein 24 kDa like protein
Relative expression level
0
1
2
3
4
5
6
7
*
*
Pearl Sac
Mantle Pallial
Mantle Edge

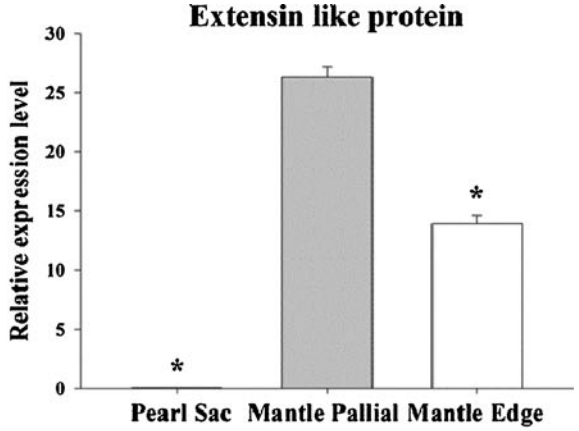
Extensin like protein
Relative expression level
0
5
10
15
20
25
30
*
*
Pearl Sac
Mantle Pallial
Mantle Edge

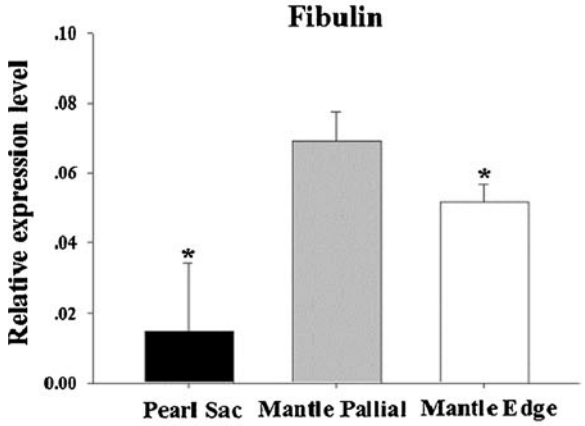
Fibulin
Relative expression level
0.00
.02
.04
.06
.08
.10
*
*
Pearl Sac
Mantle Pallial
Mantle Edge

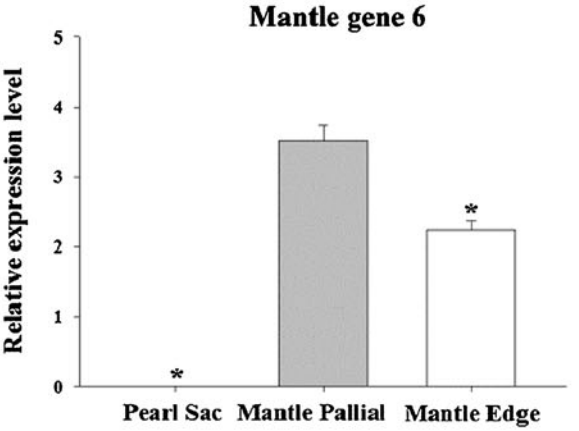
Mantle gene 6
Relative expression level
0
1
2
3
4
5
*
*
Pearl Sac
Mantle Pallial
Mantle Edge

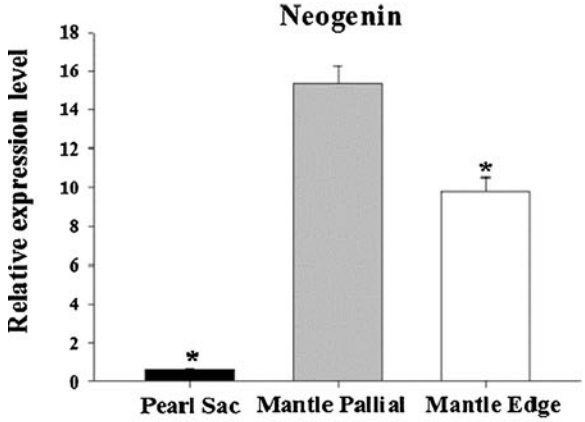
Neogenin
Relative expression level
0
2
4
6
8
10
12
14
16
18
*
*
Pearl Sac
Mantle Pallial
Mantle Edge

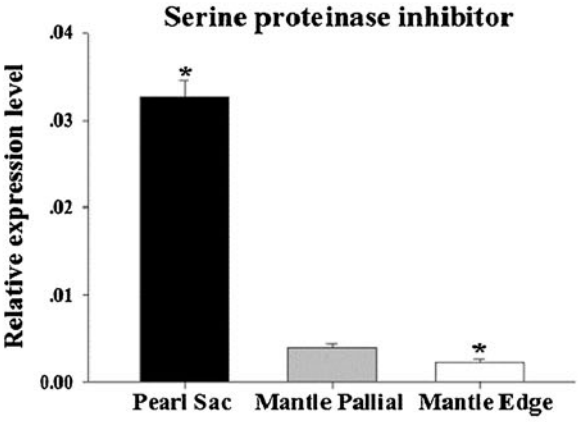
Serine proteinase inhibitor
Relative expression level
0.00
.01
.02
.03
.04
*
*
Pearl Sac
Mantle Pallial
Mantle Edge

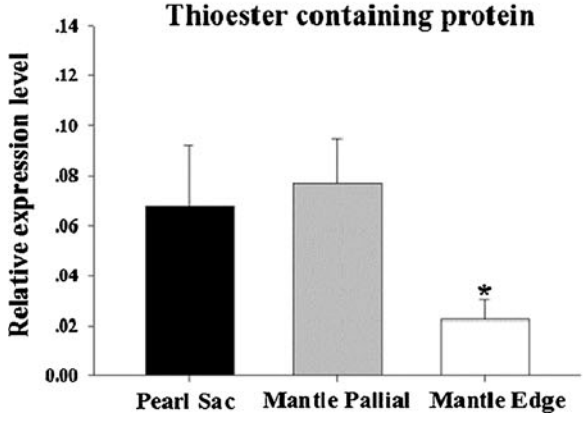
Thioester containing protein
Relative expression level
0.00
.02
.04
.06
.08
.10
.12
.14
*
Pearl Sac
Mantle Pallial
Mantle Edge

◀ **Fig. 3** The expression levels of eight genes selected from mantle pallial SSH cDNA library in the pearl sac, oyster mantle pallial, and mantle edge as determined by real-time PCR. Each value represents the mean ± SE of three samples each from three individuals. The values are normalized by those of the GAPDH gene. *Asterisk* indicates a significant difference of the gene expression in sample tissues from that in mantle pallial ($P<0.05$)

genes critical for pearl formation. Interestingly, so far as we know, this is the first time to report the homologous pearl formation genes found between bivalve and gastropod molluscans. For a long time, there has been no data supporting the evolutionary relationship of pearl formation between bivalve and gastropod species. Some researcher even suggested that nacre building genes were in parallel evolution (Jackson et al. 2010). In fact, only AP24-like protein gene was detected in mantle pallial SSH cDNA library while lustrin A and perlwapin-like protein gene were exclusively present in the mantle edge SSH cDNA library. The discrepancy of their expression in mantle regions made the validation of the functional roles of these three genes more meaningful to clarify the evolutionary study of molluscan nacre formation.

As mentioned at the very beginning of the discussion, gene expression in mantle pallial favored its functioning in nacre secretion and it also may direct $CaCO_3$ biomineralization that should almost declare their putative roles in pearl formation. In fact, EF hand calcium-binding protein gene, mantle gene 4, and other oyster biomineralization genes were covered in our mantle pallial SSH cDNA library and their dominant expression in mantle pallial were proved at the same time.

Furthermore, 36 unique ESTs in the mantle pallial SSH cDNA library showed a great potential in governing pearl formation in the gene ontology analysis. Functionally, six EST-encoding genes possess calcium-binding capacity and their further study will highlight the metabolic mechanism of calcium ions supplying pearl formation. The gene ontology analysis in the term of cellular component indicated that the expressed proteins of these genes would not directly participate in pearl formation but function inside cells maintaining the balance of calcium ions in oyster bodies. In the view of biological process, these genes are related to biological regulation. Therefore, these genes perhaps mainly act on the upstream genes in the whole signaling pathway of the genetic regulation for pearl formation. The sequence data of the present cDNA library provided lots of issues for further study.

To prove the associations between the identified genes and pearl formation, candidate genes were examined for their expression in pearl sac. All the test genes showed amplifiable expression in this pearl biogenic region, suggesting their involvement in pearl formation. The differential gene expression in mantle pallial and pearl sac suggests a complicated regulatory mechanism after a mantle pallial is transplanted to host oysters. This is consistent with our previous expression analysis of other known nacre formation genes (Wang et al. 2009). Immune rejection perhaps is one of the main reasons for downregulation of pearl formation genes in pearl sac. Strikingly, the serine proteinase inhibitor gene exhibited higher expression levels in pearl sac than reference mantle pallials, indicating its important contribution to pearl formation.

Finally, it should not ignore the genes screened out by the mantle edge SSH cDNA library. The homology of the ESTs with aspein, ferritin-like protein, shematrin, tyrosinase, and other novel biomineralization genes suggests that more characterization of these genes will collect important information and promote the understanding of molluscan calcite shell growth (Zhang et al. 2003; Zhang et al. 2006; Yano et al. 2006; Liu et al. 2007; Takeuchi et al. 2008).

Taken all together, in this study the pearl oyster mantle pallial and mantle edge SSH cDNA libraries were successfully constructed and displayed super capacity in the identification of pearl formation genes. The harvested sequence data provided a database for the characterization of pearl formation genes, making the further molecular mechanism research possible.

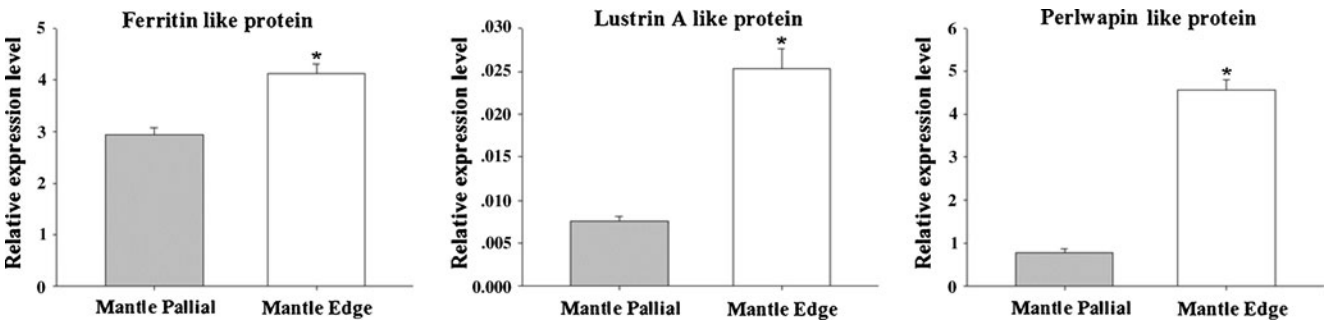


**Fig. 4** The expression levels of three genes selected from mantle edge SSH cDNA library in the oyster mantle pallial and mantle edge as determined by real-time PCR. Each value represents the mean ± SE of three samples each from three individuals. The values were normalized by those of the GAPDH gene. *Asterisk* indicates a significant difference of the gene expression in sample tissues from that in mantle pallial ($P<0.05$)

## References


Addadi L, Weiner S (1997) A pavement of pearl. Nature 389:912–915

Addadi L, Joester D, Nudelman F, Weiner S (2006) Mollusk shell formation: a source of new concepts for understanding biomineralization processes. Chem Eur J 12:980–987

Che LM, Golubic S, Le Campion-Alsumard T, Payri C (2001) Developmental aspects of biomineralisation in the Polynesian pearl oyster *Pinctada margaritifera var. cumingii*. Oceanol Acta 24:S37–S49

Checa AG, Cartwright JHE, Willinger MG (2009) The key role of the surface membrane in why gastropod nacre grows in towers. Proc Natl Acad Sci U S A 106:38–43

Diatchenko L, Lau YC, Campbell AP, Chenchik A, Moqadam F, Huang B, Lukyanov S, Lukyanov K, Gurskaya N, Sverdlov ED, Siebert PD (1996) Suppression subtractive hybridization: a method for generating differentially regulated or tissue-specific cDNA probes and libraries. Proc Natl Acad Sci U S A 93:6025–6030

Diatchenko L, Lukyanov S, Lau YC, Siebert PD (1999) Suppression subtractive hybridization: a versatile method for identifying differentially expressed genes. Methods Enzymol 303:349–380

Duplat D, Puissegur M, Bedouet L, Rousseau M, Boulzaguet H, Milet C, Sellos D, Wormhoudt AV, Lopez E (2006) Identification of calconectin, a calcium-binding protein specifically expressed by the mantle of *Pinctada margaritifera*. FEBS Lett 580:2435–2441

Falini G, Albeck S, Weiner S, Addad L (1996) Control of aragonite or calcite polymorphism by mollusk shell macromolecules. Science 271:67–69

Gong N, Li Q, Huang J, Fang Z, Zhang G, Xie L, Zhang R (2008) Culture of outer epithelial cells from mantle tissue to study shell matrix protein secretion for biomineralization. Cell Tissue Res 333:493–501

Hare PE (1963) Amino acids in the proteins from aragonite and calcite in the shells of *Mytilus californianus*. Science 139:216–217

Huang X, Madan A (1999) CAP3: a DNA sequence assembly program. Genome Res 9:968–977

Huang J, Zhang C, Ma Z, Xie L, Zhang R (2007) A novel extracellular EF-hand protein involved in the shell formation of pearl oyster. Biochim Biophys Acta 1770:1037–1044

Jackson DJ, McDougall C, Woodcroft B, Moase P, Rose RA, Kube M, Reinhardt R, Rokhsar DS, Montagnani C, Joubert C, Piquemal D, Degnan BM (2010) Parallel evolution of nacre building gene sites in molluscs. Mol Biol Evol 27:591–608

Liu H, Liu S, Ge Y, Liu J, Wang X, Xie L, Zhang R, Wang Z (2007) Identification and characterization of a biomineralization related gene PFMG1 highly expressed in the mantle of *Pinctada fucata*. Biochemistry 46:844–851

Ma Z, Huang J, Sun J, Wang G, Li C, Xie L, Zhang R (2007) A novel extrapallial fluid protein controls the morphology of nacre lamellae in the pearl oyster, *Pinctada fucata*. J Biol Chem 282:23253–23263

Meyers MA, Lin AY, Chen P, Muyco J (2008) Mechanical strength of abalone nacre: role of the soft organic layer. J Mech Behav Biomed Mater 1:76–85

Michenfelder M, Fu G, Lawrence G, Weaver JC, Wustman BA, Taranto L, Evans JS, Morse DE (2003) Characterization of two molluscan crystal-modulating biomineralization proteins and identification of putative mineral binding domains. Biopolymers 70:522–533

Miyamoto H, Miyashita T, Okushima M, Nakano S, Morita T, Matsushiro A (1996) A carbonic anhydrase from the nacreous layer in oyster pearls. Proc Natl Acad Sci U S A 93:9657–9660

Perrigault M, Tanguy A, Allam B (2009) Identification and expression of differentially expressed genes in the hard clam, *Mercenaria mercenaria*, in reponse to quahog parasite unknown (QPX). BMC Genomics 10:377

Roberts S, Goetz G, White S, Goetz F (2009) Analysis of genes isolated from plated hemolytic of the Pacific oyster, *Crassostreas gigas*. Mar Biotechnol 11:24–44

Rousseau M, Lopez E, Cute A, Mascara G, Smith DC, Maslin R, Borate X (2005) Sheet nacre growth mechanism: a Verona model. J Struct Biol 149:149–157

Samata T, Hayashi N, Koon M, Hasegawa K, Hornito C, Akers S (1999) A new matrix protein family related to the nacreous layer formation of *Pinctada fucata*. FEBS Lett 462:225–229

Sanchez S, Hordes S, Allier FH (2007) Identification of proteins involved in the functioning of *Raffia pachyptila* symbiosis by subtractive suppression hybridization. BMC Genomics 8:337

Schefe JH, Lehmann KE, Buschmann IR, Unger T, Kaiser HF (2006) Quantitative real-time RT-PCR data analysis: current concepts and the novel "gene expression's CT difference" formula. J Mol Med 84:901–910

Shen X, Belcher AM, Hansma PK, Stucky GD, Morse DE (1997) Molecular cloning and characterization of lustrin A, a matrix protein from shell and pearl nacre of *Haliotis rufescens*. J Biol Chem 272:32472–32481

Straub PF, Higham ML, Tanguy A, Landau BJ, Phoel WC, Hales LSJ, Thwing TK (2004) Suppression subtractive hybridization cDNA libraries to identify differentially expressed genes from contrasting fish habitats. Mar Biotechnology 6:386–399

Sudo S, Fujikawa T, Nagakura T, Ohkubo T, Sakaguchi K, Tanaka M, Nakashima K (1997) Structures of mollusc shell framework proteins. Nature 387:563–564

Suzuki M, Saruwatari K, Kogure T, Yamamoto Y, Nishimura T, Kato T, Nagasawa H (2009) An acidic matrix protein, Pif, is a key macromolecule for nacre formation. Science 325:1388–1390

Takeuchi T, Endo K (2006) Biphasic and dually coordinated expression of the genes encoding major shell matrix proteins in the pearl oyster *Pinctada fucata*. Mar Biotechnology 8:52–61

Takeuchi T, Sarashina I, Lijima M, Endo K (2008) In vitro regulation of $CaCO_3$ crystal polymorphism by highly acidic molluscan shell protein Aspein. FEBS Lett 582:591–596

Towe KM, Charles W, Harper J (1966) Pholidostrophiid Brachiopods: origin of the nacreous luster. Science 154:153–154

Treccani L, Mann K, Heinemann F, Fritz M (2006) Perlwapin, an abalone nacre protein with three four-disulfide core (whey acidic protein) domains, inhibits the growth of calcium carbonate crystals. Biophys J 91:2601–2608

Wang N, Kinoshita S, Riho C, Maeyama K, Nagai K, Watabe S (2009) Quantitative expression analysis of nacreous shell matrix protein genes in the process of pearl biogenesis. Comp Biochem Physiol B 154:346–350

Xu W, Faisal M (2009) Identification of the molecules involved in zebra mussel (*Dreissena polymorpha*) hemolytic host defense. Comp Biochem Physiol B 154:143–149

Yano M, Nagai K, Morimoto K, Miyamoto H (2006) Shematrin: a family of glycine-rich structural proteins in the shell of the pearl oyster *Pinctada fucata*. Comp Biochem Physiol B 144:254–262

Zhang C, Zhang R (2006) Matrix proteins in the outer shells of molluscs. Mar Biotechnology 8:572–586

Zhang Y, Meng Q, Jiang T, Wang H, Xie L, Zhang R (2003) A novel ferritin subunit involved in shell formation from the pearl oyster (*Pinctada fucata*). Comp Biochem Physiol B 135:43–54

Zhang C, Xie L, Huang J, Chen L, Zhang R (2006) A novel putative tyrosinase involved in periostracum formation from the pearl oyster (*Pinctada fucata*). Biochem Biophys Res Commun 342:632–639